Published in final edited form as:
Deep Sea Res Part 2 Top Stud Oceanogr. 2014 May ; 103: 40–54. doi:10.1016/j.dsr2.2012.11.001.

Spatial and temporal variability of *Alexandrium* cyst fluxes in the Gulf of Maine: Relationship to seasonal particle export and resuspension

C.H. Pilskaln[a,*], **D.M. Anderson**[b], **D.J. McGillicuddy**[b], **B.A. Keafer**[b], **K. Hayashi**[a], and **K. Norton**[b]

[a]School for Marine Science and Technology, University of Massachusetts Dartmouth, New Bedford, MA 02744, USA

[b]Woods Hole Oceanographic Institution, Woods Hole, MA 02543, USA

Abstract

Quantification of *Alexandrium* cyst fluxes through the Gulf of Maine water column is central to understanding the linkage between the source and fate of annual *Alexandrium* blooms in the offshore waters. These blooms often lead to paralytic shellfish poisoning (PSP) and extensive closures of shellfish beds. We report here on time-series sediment trap deployments completed at four offshore locations in the gulf between 2005 and 2010 as components of two ECOHAB–GOM field programs. Data presented documents the substantial spatial and temporal fluctuations in *Alexandrium fundyense* cyst fluxes in the gulf. Cyst delivery out of the euphotic zone peaked primarily between July and August following annual spring–summer *Alexandrium* blooms and was greatest in the western gulf. At all sites, cyst flux maxima to the subsurface waters were rarely coincident with seasonal peaks in the total mass export of particulate material indicating that cyst delivery was primarily via individually sinking cysts. Where persistent benthic nepheloid layers (BNLs) exist, significant sediment resuspension input of cysts to the near-bottom water column was evidenced by deep cyst fluxes that were up to several orders of magnitude greater than that measured above the BNL. The largest cyst fluxes in the BNL were observed in the eastern gulf, suggesting greater resuspension energy and BNL cyst inventories in this region. Temporal similarities between peak cyst export out of the upper ocean and peak cyst fluxes in the BNL were observed and document the contribution of seasonal, newly formed cysts to the BNL. The data however also suggest that many *Alexandrium* cells comprising the massive, short-lived blooms do not transition into cysts. Time-series flow measurements and a simple 1D model demonstrate that the BNL cyst fluxes reflect the combined effects of tidal energy-maintained resuspension, deposition, and input of cysts from the overlying water column.

Keywords

Gulf of Maine; Particulate flux; Sediment traps; *Alexandrium*; Cysts; Resuspension

*Corresponding author: cpilskaln@umassd.edu (C.H. Pilskaln).

1. Introduction

The Gulf of Maine (GOM) is well-known for elevated levels of primary and secondary production, resulting in an abundance of shellfish, finfish and marine mammal biomass (Bigelow, 1926; Shumway et al., 1988; Townsend, 1991; Pershing et al., 2005). This productive shelf sea, and the adjacent Bay of Fundy, is also characterized by the occurrence of seasonal harmful algal blooms (HABs) of the neurotoxin-producing dinoflagellate *Alexandrium fundyense*, hereafter termed *Alexandrium* (Anderson, 1997; Martin et al., 2005). The ecology and oceanography of these HAB species have been relatively well studied through the NOAA/NSF Ecology and Oceanography of Harmful Algal Blooms (ECOHAB) Program (Anderson et al., 2005c). Annual *Alexandrium* blooms in the Gulf of Maine during the spring-early summer months and have been well-documented since the 1990s (Anderson, 1997; Anderson et al., 1994; Townsend et al., 2001; Keafer et al., 2005a,b; McGillicuddy et al., 2005; Townsend et al., 2005). Even though *Alexandrium* typically represents a very small percentage of the total spring–summer bloom phytoplankton assemblage, the ingestion by plankton and shellfish of toxin-containing cells and cysts can result in a substantial negative impact on the health of higher trophic level organisms, including humans (Turner and Borkman, 2005; Turner et al., 2005; Hoagland and Scatasta, 2006; Townsend et al., 2010). Additionally, the settling and accumulation of dormant *Alexandrium* cysts in Gulf sediments provides for a continuous cycle of yearly blooms in the region (Anderson et al., 2005a).

Alexandrium encystment and excystment dynamics have been detailed by Anderson et al. (2005a). It is believed that germination from the dormant cyst stage to the vegetative cell stage initiates the planktonic blooms, which are facilitated by favorable nutrient concentrations (specifically high inorganic nitrogen levels) and increasing temperature and light conditions (Anderson, 1980, 1998; Etheridge and Roesler, 2005; Love et al., 2005; Matrai et al., 2005; Townsend et al., 2005). In turn, the water column transformation of asexual vegetative cells to sexually-reproducing gametes is believed to be induced by decreasing nutrient, temperature and light levels in the late summer and early fall (Dale, 1983; Anderson and Keafer, 1985; Anderson, 1998; Anderson et al., 2005a; Kirn et al., 2005). Sexual fusion of gametes results in the formation of a planozygote cell, which transforms within approximately a week into a hypnozygote cyst that remains dormant for a minimal period of 2–6 months (Anderson, 1988). Sedimentary accumulation of the dormant cysts in the Gulf of Maine (and the Bay of Fundy) has been shown to be widespread along the coast as well as offshore (Lewis et al., 1979; Anderson et al., 2005a, 2014).

Since 2004, ECOHAB studies (ECOHAB-GOM and GOMTOX) have produced large-scale surveys of *Alexandrium* distributions and maps of benthic cyst abundance (Townsend et al., 2001, 2005; Anderson et al., 2005a,b,c; Keafer et al., 2005a,b; Anderson et al., 2014). The water column and sediment distributions of *Alexandrium* cells and cysts suggest that a very large cyst seed-bed in the Bay of Fundy (BOF) is a source of recurrent spring-summer blooms that feed the Maine Coastal Current (MCC) (Townsend et al., 2001; Anderson et al., 2005a; McGillicuddy et al., 2005; Pettigrew et al., 2005). Another cyst bed offshore of Casco and Penobscot Bays is hypothesized to be an additional source of *Alexandrium* blooms occurring in the western GOM and Massachusetts Bay region via the western

segment of the MCC, transporting *Alexandrium* to the west and south (McGillicuddy et al., 2003, 2005; Anderson et al., 2005a,b; Pettigrew et al., 2005; Townsend et al., 2005).

The purpose of the current communication is to report on the measured time-series fluxes of *Alexandrium* cysts through the water column at several locations in the offshore regions of the western and eastern Gulf of Maine. The data sets were collected in ECOHAB field programs spanning five years (2005–2010). Our objectives in making the time-series measurements were to provide a temporal connection between the near-surface *Alexandrium* blooms and the delivery of sinking cysts to sub-euphotic depths and the underlying sediments, and to examine the relationship of cyst fluxes to the seasonal mass flux of particulate material. Understanding the timing and magnitude of *Alexandrium* cyst fluxes and the temporal and spatial dynamics of their movement (i.e., sinking, resuspension, etc.) are presently not included in Gulf of Maine *Alexandrium* bloom forecast models (He et al., 2008; Li et al., 2009). However, water column cyst fluxes provide the link between bloom senescence and the formation of underlying sedimentary seed-beds which provide the inoculum for the annual blooms and as such represent a significant factor that should be included in the forecast models.

2. Methods

High-resolution, time-series sediment traps (model Mark 7, McLane Research Labs, Inc.; Honjo and Doherty, 1988; Honjo et al., 2000; Pilskaln et al., 1996, 2004) were deployed on subsurface moorings at two depths, at four sites between 2005 and 2010 as field components of two NOAA ECOHAB programs: Cyst Dynamics I (2004–2007) and GOMTOX (2006–2011). The former project's mooring work was focused in the eastern Gulf and the latter (GOMTOX) was focused in the western Gulf. The mooring locations were north-central Jordan Basin (JB, 12 months: 2005–2006), offshore Penobscot Bay (PB, 18 months: 2005–2006), northern Stellwagen Bank (SB, 12 months: 2007–2008) and northern Wilkinson Basin (WB, 26 months: 2008–2010) (Fig. 1; Table 1). The traps had a baffled surface collection area of 0.5 m^2 and collected time-series samples in thirteen 250 ml volume cups per deployment. Prior to deployment, trap cups were pre-poisoned with an 8% density-adjusted formalin solution in filtered seawater buffered to a pH of 8.0–8.1. Recovery and redeployment of the trap moorings occurred approximately every 5–9 months with individual cup collection periods varying from ~10–21 days. The traps were programmed to insure that per deployment period, the cups on the upper and lower traps rotated and collected sinking particulate material on the same time interval.

Particulate sample handling and processing followed the standard procedures detailed in Pilskaln and Paduan (1992) and Pilskaln et al. (2004). Immediately following trap recoveries, sample cup supernatant pH values were recorded, additional buffered formalin solution was added and all samples were refrigerated stored at 4 °C. Total cup samples were gently washed with filtered seawater through 1 mm and 500 μm Nylon mesh sieves to remove crustacean and molluscan swimmers (e.g., copepods, euphausids, amphipods and pteropods), and the remaining particulate sample material was quantitatively split into quarters using a four-section wet splitter (McLane Research labs, Inc.). Two wet splits were filtered, dried and weighed for mass flux determination and dried ground subsamples were

analyzed for particulate organic carbon composition (POC) using standard coulometric carbon analysis techniques (Pilskaln et al., 1996, 2004).

One 1/4 wet split was set aside and processed for *Alexandrium* cyst counting. If the volume of particulate material in the split was minimal, the full volume of the split was processed. If the particulate volume was high, then a known volume of the split was removed for further processing. The subsamples were initially sieved through a 20 μm Nylon mesh sieve with filtered seawater to concentrate the cysts and to remove the formalin solution. The >20 μm particulate fraction containing the cysts was retained on the sieve and further processed using standard cyst concentrating protocols (Anderson et al., 2003; Anderson et al., 2005a). Briefly, the samples were resuspended off the 20 μm sieve into 45 ml of filtered seawater and sonified for 60 s. The disaggregated sample was sieved to remove fine material of <20 μm, and the >20 μm fraction with cysts was resuspended into 14 ml of filtered seawater. For primuline staining of the cysts, the sample was centrifuged, the seawater was removed by aspiration, and the resulting pellet of centrifuged cysts was resuspended into cold methanol and stored for at least 24 h. The sample was centrifuged again, the methanol removed, and the pellet resuspended in 10 ml of distilled water. After centrifugation, 2 ml of primuline stock (2 mg ml^{-1}) was added directly to the pellet and incubated at 4 °C for 1 hour. The stained sample was centrifuged, excess primuline removed, and the pellet resuspended in a final known volume of distilled water (usually 5–10 ml). One ml of the processed sample was loaded into a Sedgewick-Rafter chamber and the green fluorescently-stained cysts were counted at 10x with a Zeiss epi-fluorescent microscope (excitation=450–490 nm BP; emission=510 nm LP). The number of cysts per trap was calculated from the known volumes of each step during the processing and the fraction of the whole sample represented by the split. Only intact, pigmented cysts were counted; empty cysts were not quantified.

A lack of sub-surface, time-series current velocity measurements for our trap sites coupled with the potential impact of lateral flow on the total particulate and cyst fluxes necessitated the collection of current measurements at the trap depths. Our specific objective in making coincident flow speed and direction measurements at the trap depths was to determine if sustained flows of ≥20 cm s^{-1} were present which could lead to an under-sampling bias of small settling particles, including cysts (Gardner, 1980a,b). Aquadopp (Nortek, USA) acoustic current meters were mounted on the trap frames at SB, WB and JB sites such that the acoustic sensor head was flush with the trap collection surfaces. The symmetrical configuration of the acoustic sensors directed the beams over the baffled trap collection surface, with the center of the measurement volume located 53 cm above the trap surface (actual measurement distance was 26–79 cm above traps). This configuration minimized disturbance of the beams by the plastic trap bridle components. Data collection frequency varied from 30–90 min, depending on deployment period and site. Upon recovery of the moorings, the current meter data was immediately downloaded from the instruments into a standard spreadsheet as directed in the instrument manual. To isolate subtidal and tidal currents, each data set was passed through a 33-h low-pass filter (i.e., second-order Butterworth filter; Butterworth, 1930). The low-pass filter preserves the phase of the original signal and smoothes the data providing an assessment of lower-frequency flows, essentially eliminating variability due to tides or other processes with time scales of <33 h.

This subtidal signal output from the filter process was subtracted point-by-point from the original data resulting in a residual time-series comprised of higher-frequency processes with time scales of <33 h representing the tidal energy band or tidal currents.

The JB flow data set presented here was collected between Aug. 2010 and May 2011 (as part of a non-ECOHAB field project) and thus was not coincident with the JB 2005–2006 trap deployments. Because our current meter instruments were not obtained until after 2006, in situ current flow measurements were not available at the 2005–2006 JB and PB sites. However, the 2010–2011 JB flow data does provide valuable information on the currents occurring over a 9-month period at the exact 2005–2006 JB sediment trap depths and location.

Characterization of the general hydrographic features at the mooring sites were obtained when possible from calibrated CTD and transmissometer profiles completed on several mooring recovery/redeployment cruises and additional Gulf of Maine ECOHAB/ *Alexandrium* survey cruises.

3. Results

We observed significant temporal and spatial variability in the *Alexandrium* cyst fluxes. Over the five-year study period, 2–5 orders of magnitude range in fluxes were observed at each site, either as a function of depth or time. Table 2 provides the minimum, maximum and median cyst flux measured at each site and depth. Due to the wide range in cyst fluxes at any one site and depth, median values are much more useful than mean or standard deviation values when comparing sites. Despite the extreme range in values, flux patterns do emerge from the time-series data sets for each site and depth. Site-specific results are presented below beginning with the first-collected data set and most eastern data set (JB) and progressing to the most recent western gulf data set (WB).

3.1. Jordan Basin

The 2005–2006 twelve-month cyst flux time-series measured at 150 m and 255 m in the 280 m-deep, north-central Jordan Basin is shown in Fig. 2. Cyst fluxes of 460–670 cysts m^{-2} d^{-1} at 150 m were observed in July–early August 2005, with no cysts collected in the majority of the April 2005–2006 biweekly trap samples (Fig. 2a). The 255 m cyst fluxes were substantially greater than those at 150 m and displayed high variability, a clear indication of significant sediment resuspension input (Fig. 2b). All JB 255 m trap cups contained cysts. At both depths a cyst flux peak was seen in July–early August 2005 reflecting a single delivery pulse of cysts from the upper to the deep water column (Fig. 2a and b). However the peak upper trap cyst flux of ~1000 cysts m^{-2} d^{-1} in mid-July represented one-third of the early August peak deep trap cyst flux of 3000 cysts m^{-2} d^{-1}, thus indicative of significant resuspension input of cysts to the 255 m trap. The largest 255 m cyst flux actually occurred in May 2005 when no cysts were collected at 150 m but when two particularly strong northeastern storm events occurred in the Gulf of Maine (Butman et al., 2008). The May storms may have induced resuspension of eastern gulf shelf sediments and cysts followed by possible advection to the deep offshore basin.

A gulf-wide water column survey of *Alexandrium* completed in May 2005 and subsequent 2005 summer month surveys in the western gulf showed a substantial *Alexandrium* bloom extending from the western Gulf of Maine (WGOM) to mid-coast Maine and persisting until July (Anderson et al., 2005b). The highest May surface cell concentrations of $>10^3$ cells l^{-1} were observed in WGOM/Massachusetts Bay as compared to values of <20 cells l^{-1} measured in the surface waters of Jordan Basin (Anderson et al., 2005b). The lack of cysts in the JB 150 m spring 2005 trap samples was likely due to the fact that the bloom did not extend into the offshore eastern gulf until later in the summer.

Total mass flux (TMF) of particulates at JB 150 m consisted of planktonic detrital material produced in the overlying water column as well as fine lithogenic material adhered to and incorporated into aggregated organic matter (Pilskaln, 2009). Highest TMF values were observed at JB 150 m in May 2005 and March 2006, following or coincident with the annual spring phytoplankton bloom period (Fig. 2c). Secondary 150 m particle export peaks were observed in early and late fall months and related to the annual, large fall phytoplankton bloom occurring in Gulf waters (Fig. 2c; Thomas et al., 2003; Pilskaln, 2009; Townsend and Ellis, 2009). Particulate organic carbon flux to 150 m displayed a similar seasonal pattern (Pilskaln, 2009). The 150 m July–early August cyst flux peak of ~500 cysts m^{-2} d^{-1} occurred just before the moderate TMF peak at 150 m in late August–early September. This suggests that the cysts primarily settled as individually out of the surface with minimal cyst incorporation into planktonic-derived, sinking detrital material comprising the early fall mass flux event.

Particle mass flux measured at 255 m was 2-orders of magnitude larger than that at 150 m, providing strong evidence of high, near-bottom particle resuspension input to the deeper trap (Fig. 2d). CTD/transmissometer profiles from the mooring site collected in the spring and fall on several mooring cruises show clear evidence of a thick benthic nepheloid layer (BNL) beginning at approximately 200 m as evidenced by a doubling of the beam attenuation between 200 and 280 m (Fig. 3a). The location of the 150 m trap was at the lower boundary of the clear mid-water region and the 255 m trap was situated in the core of the BNL. The existence of a thick, year-round BNL in deep Jordan Basin has been previously documented by a number of researchers (Spinrad, 1986; Townsend et al., 1992; Pilskaln et al., 1998; Kirn et al., 2005; Pilskaln et al., 2006). The highest BNL cyst flux in the time-series occurring in May coincided with a TMF peak at 255 m. Although a regression analysis of the 255 m time-series cyst and TMF fluxes results in a low r^2 value, the temporal patterns are broadly similar, i.e., several peaks in the late spring to August, decreasing fluxes in August–September, and flux increases in November followed by lower December–January values (Fig. 2b and d). These data suggest multiple events of bottom resuspension input of cysts to the BNL-deployed trap, coupled with the summer delivery from the overlying water column.

Summarized records (=9 months of 30 min frequency data obtained from August 2010 to May 2011) of the tidal, subtidal and total flow speeds and direction at 150 m and 255 m at the JB mooring site are displayed as rose diagrams in Fig. 4. Rose diagrams separate the measurements into directional ‘petals’ (each petal is a 22.5° slice) as well as velocity bins represented by the gray-scale shading within each petal. The percentage of time the

measured flows fell within a specific direction and velocity bin is indicated by the annular circles of the rose diagrams. At the JB site, diurnal tidal currents dominated the total signal and were oriented along a N–NE/S–SW axis at both depths. Subtidal, residual circulation flow was fairly weak, never exceeding 10 cm s^{-1} and the lack of a dominant subtidal flow direction was a reflection of the cyclonic gyre centered over Jordan Basin (Brooks and Townsend, 1989; Lynch et al., 1997; Pettigrew et al., 2005). Approximately 75% of our flow measurements at 150 m in north-central Jordan Basin were <20 cm s^{-1}; at 255 m depth, 80% of the tidally dominated flow was less than 20 cm s^{-1}.

3.2. Offshore Penobscot Bay

The PB site (bottom depth 150 m) was located on the far eastern edge of the western Gulf of Maine region, within a region where an offshore turning of the coastal current has been documented (Brooks and Townsend, 1989; Lynch et al., 1997; Pettigrew et al., 2005) (Fig. 1). An 18-month cyst flux time-series was obtained at 75 m and 135 m from April 2005 to October 2006; individual sample collection frequency was biweekly (Fig. 5). The May–July 2005 bloom of *Alexandrium* in the western Gulf was clearly reflected in a large cyst flux peak at 75 m (2000 cysts m^{-2} d^{-1}) and at 135 m (12,000 cysts m^{-2} d^{-1}) in July–early August 2005 (Fig. 5a and b). The temporal link between the July peak cyst fluxes at 75 m and 135 m following the summer 2005 *Alexandrium* bloom implies a maximum 2-week (=trap cup sampling frequency) transit time between the two depths or a 5 m d^{-1} cyst sinking rate.

Comparing the 75 m cyst and TMF patterns, the July–early August 2005 cyst flux maxima occurred approximately 2 months after the May peak in TMF flux (Fig. 5 and c). The TMF at 75 m was highly correlated to measured POC fluxes (r^2=0.8), suggesting production and grazing control of the timing and magnitude of the mass delivery of particle matter to the subsurface (Pilskaln, 2009). The temporal decoupling between the 75 m cyst flux and TMF peaks in spring–summer 2005 indicates that delivery of cysts to depth was not associated with the May export of planktonic organic matter (Fig. 5a and c). Cyst delivery to 75 m was low or absent throughout the remaining months of 2005 when *Alexandrium* disappears from the surface waters (Anderson, 1997; Anderson et al., 2005b). However, increasing cyst fluxes to 75 m were observed in late September–early October 2006 (Fig. 5a) coincident with a fall TMF peak at 75 m (Fig. 5c) but occurring months after a spring 2006 *Alexandrium* bloom (Li et al., 2009). The results suggest that *Alexandrium* may have remained in the region's surface waters longer in 2006 versus 2005, underwent encystment in fall 2006, and settled through the water column with the bulk of the detrital mass flux resulting from the fall bloom. The maximum delivery of total particulates to PB 75 m was an order of magnitude greater than that measured at JB 150 m (Figs. 2c and 5c), likely a reflection of the overall higher particle export at the shallower-shelf PB site located within the coastal current as compared to the JB site situated in an offshore basin and within the center of a cyclonic gyre (Pettigrew et al., 2005).

Similar to the JB site observations, cyst fluxes to the deeper PB trap were never zero and were substantially larger than those measured in the shallower trap (Fig. 5b). The PB 135 m cyst fluxes were 3 to 4-fold higher than that measured at PB 75 m, reflecting significant

resuspension input of cysts at this depth (Fig. 5a and b). The CTD/transmissometer profiles from the PB site show the top of a moderately strong BNL at ~75–80 m, with the 135 m trap deployed well-within the near-bottom particle resuspension layer (Fig. 3b). High particle resuspension input to the 135 m trap was evidenced by the 4-fold greater mean TMF measured at 135 m as compared to 75 m (Fig. 5c and d). The large May TMF peaks at both trap depths represents translation through the water column of fast-settling, organic particulates resulting from spring bloom production and grazing activities, coupled with fine sediment resuspension input generated by two substantial May 2005 storms reported by Butman et al. (2008). Total mass fluxes are often enhanced with depth via passive physical scavenging of suspended lithogenic particles (clays and fine silt) onto sinking, organic-rich detrital material. This process provides ballast and thus increases the mass density of settling organic detritus (Honjo, 1982; Pilskaln et al., 1996; Passow and De La Rocha, 2006).

3.3. Northern Stellwagen Bank

Traps were deployed at 50 m and 115 m in a 130–150 m deep basin at the northern edge of Stellwagen Bank for 12 months from May 2007 to April 2008 (12-day cup collection frequency over time-series). The location was selected as part of the first phase of the ECOHAB/GOMTOX field program (2006–2011) where the focus was on *Alexandrium* dynamics in the far western Gulf of Maine/Stellwagen region and potential impacts on offshore shell-fish beds. The SB 50 m cyst fluxes were extremely small (<10 cysts m^{-2} d^{-1}) and often zero throughout the year (Fig. 6a). No cyst flux signal was associated with the 50 m TMF flux peak in May 2007 (Fig. 6c) and the largest value of only 35 cysts m^{-2} d^{-1} was observed at the end of November–early December 2007 (point centered on 12/1/2007 on Fig. 6a). The latter was approximately one month later than the fall TMF peak at 50 m indicating a decoupling between the sinking of cysts and the major seasonal transfer of upper water column-derived particulate matter (Fig. 6a and c).

In comparison, the SB 115 m cyst fluxes were much greater, than those at 50 m although relatively low compared to the more eastern PB and JB site cyst fluxes (Figs. 2c, 5c and 6c). A mid-August to early October cyst flux peak of 2300–4900 cysts m^{-2} d^{-1} was measured at 115 m, with values decreasing to <100 by early 2008 (Fig. 6b). Approximately 50% of the SB 115 m fluxes were ≥100 cysts m^{-2} d^{-1}, with 3 of the 26 samples being devoid of cysts (Fig. 6).

The total mass flux of sinking particulates at 115 m was in general an order of magnitude higher than that at 50 m over the time-series (Fig. 6c and d), indicative of strong particle resuspension in the near-bottom. Total mass flux and POC fluxes at SB were highly correlated at the two trap depths (r^2=0.9) with major export peaks occurring in May and October/November (not shown). However, the deep cyst flux peak occurred in mid-August to mid-September and the broad 115 m TMF peak was recorded approximately a month later. This is puzzling in light of the fact that no cyst delivery from the overlying water column to SB 115 m occurred in August–September, and that bottom resuspension clearly influenced the 115 m TMF. In the absence of a temporal connection with cyst supply from the upper water column or a simultaneous bottom resuspension signal in the deep TMF, the source of the August–September 115 m cyst flux peak is unknown.

A 12-month (April–May) record of the tidal, subtidal and total flow speeds and direction at SB 50 m and SB 115 m are displayed in Fig. 7. Data collection frequency varied from 60 to 90 min. At 50 m, southeastward flowing subtidal currents primarily ≤10 cm s^{-1} but occasional flows of 10–20 cm s^{-1} were observed. Tidal currents of 10–20 cm s^{-1} were aligned southeast–northwest (Fig. 7). The total signal at 50 m reveals a subtidal-dominant flow. At 115 m, southeast-northwest tidal flow dominated the total signal with weak, <10 cm s^{-1} subtidal flows to the southeast (Fig. 7). Ten percent of the measured velocities at 50 m were ≥20 cm s^{-1} over the time-series; 5% of the 115 m velocities were ≥20 cm s^{-1}.

3.4. Wilkinson Basin

The longest particle export and cyst flux time-series from sediment traps was obtained at the northern Wilkinson Basin (WB) site (Fig. 1). Twenty-six months of data (August 2008–October 2010) from 95 and 180 m is shown in Fig. 8. Trap cup sampling periods varied over the 2008–2010 time period from 3 weeks per cup (August 2008–June 2009), 2 weeks per cup (October 2009–June 2010) and 10 days per cup (June 2009–October 2009 and June 2010–October 2010). Notably large cyst flux peaks occurred between the months of July and September in 2009 and 2010 (Fig. 8a and b). The substantial July 2009 cyst flux peaks at WB (e.g., 75,236 cysts m^{-2} d^{-1} at 95 m and 292,894 cysts m^{-2} d^{-1} at 180 m) followed a massive 10-day bloom of *Alexandrium* documented off New Hampshire and southern Maine (McGillicuddy, unpublished) and represents the highest observed cyst fluxes to date in the Gulf of Maine. The trap sampling frequency of 10 days during July–September 2009 and 2010, coupled with the high degree of temporal coherence observed between the maximum cyst fluxes at the two trap depths, results in an estimated cyst sinking rate of 9 m d^{-1} between 95 and 180 m (Fig. 8).

The seasonal pattern of particle export in the upper water column at 95 m in Wilkinson Basin displayed fall TMF peaks as were observed at JB 150 m and PB 75 m. The July 2009 TMF peak was coincident with cyst flux peaks at 95 m and 180 m, thus demonstrating the important influence of the massive bloom on the TMF (Fig. 8a–c). Major differences in the temporal flux pattern at WB as compared to the more eastern trap sites were that winter (December–January) TMF peaks were documented in 2009 and 2010 at WB 95 m (attributed to an elevated input of *Limacina retroversa* pteropod shells; Pilskaln, 2009; Hayashi, unpublished) and there was a lack of late spring TMF peaks (Fig. 8c).

As seen at the other sites, the deep trap cyst and TMF fluxes were substantially greater than that measured by the shallower, upper trap. At WB, there was an order of magnitude mean increase in such fluxes between the upper and deeper traps (Fig. 8c and d). Transmissometer evidence of a well-defined BNL in Wilkinson Basin has been provided in previous studies (Spinrad, 1986; Townsend et al., 1992; Pilskaln et al., 1998; Packard and Christensen, 2004; Kirn et al., 2005; Pilskaln et al., 2006) and was observed in the present study at the WB mooring site where the 180 m trap was located in the top region of the near-bottom nepheloid layer (Fig. 3).

Twenty-two months of integrated current flow speed and direction data (30 min-interval sampling rate) from WB 95 m and 180 m is shown in Fig. 9. At 95 m the flow was comprised of a combination of NW–SE aligned tidal currents of 10–20 cm s^{-1}, and a

relatively weak subtidal flow component directed to the south–southwest with a mean speed of ≤10 cm s^{-1}. At 180 m, NW–SE-trending tidal currents dominated and were primarily between 10–20 cm s^{-1}.

4. Discussion

4.1. Seasonal and inter-annual cyst delivery through the water column

The cyst flux data sets presented document a summer-focused cyst delivery to subsurface waters following the annual blooms of *Alexandrium* in the Gulf of Maine. Twelve to twenty-four month data sets from the JB, PB and WB sites in particular show a seasonal cyst export pattern of a sharply defined summer peak, which was repeated year to year. Cyst delivery to the upper sediment traps (at 50–150 m depth depending on the site) following the blooms involves a complex mixture of spatial and temporal processes. There is potential for horizontal dispersion of cysts that sink at a laboratory-measured rate of 6–11 m d^{-1} (Anderson et al., 1985; Townsend et al., 2005; Turner and Borkman, 2005). Using the analysis presented in Siegel and Deuser (1997) and assuming a current of 10–15 cm s^{-1}, which represents the speed observed in the vast majority of our time-series flow measurements at the sites, a cyst sinking at 10 m d^{-1} from the surface waters might be transported laterally a distance of several 10's of kms to over 100 km before reaching a trap depth between 50 m and 150 m, respectively. *Alexandrium* blooms documented in the Gulf of Maine often extend over 100–200 km (Townsend et al., 2001). Lateral transport of sinking cysts that have formed in the surface waters likely displaces a substantial amount of cysts downstream of the bloom. However, the uppermost traps located at appreciable sub-euphotic depths do reflect the peak collection of sinking cysts following the bloom period, regardless of potential lateral advection or geographic proximity of the traps relative to the highest *Alexandrium* surface cell concentrations.

Major unknowns in predicting the formation of cysts is the rate at which *Alexandrium* cells transform from asexual vegetative cells to sexual gametes, plus the probability that gamete encounter rate will be great enough to lead to successful fusion, planozygote formation and encystment. Intense blooms occurring in the Gulf of Maine (and the Bay of Fundy) where the *Alexandrium* cell concentrations in the surface waters routinely reach10^4–10^6 cells l^{-1}, represent events in which a critical gamete density threshold is likely achieved, resulting in the formation of abundant cysts that re-supply underlying benthic cyst seed-beds (White and Lewis, 1982; Martin and White, 1988; Townsend et al., 2001; Kirn et al., 2005). Biological factors coupled with circulation dynamics, which help concentrate gametes, will ultimately determine mating success, cyst formation and cyst flux to sub-euphotic depths.

Comparison of the GOM cyst fluxes in the upper water column to those reported from shallow (11–25 m), 2-year time-series coastal sediment trap deployments off Japan and in the Mediterranean reveals a much wider range of maximum flux values for the Gulf of Maine. Montresor et al. (1998) reported a maximum daily *Alexandrium* cyst flux at 25 m of 50,000 cysts m^{-2} occurring in July–September in the Gulf of Naples; Fugii and Matsuoka (2006) reported a maximum in May–June of 6000 *Alexandrium* cysts m^{-2} d^{-1} at 11 m depth in Omura Bay at the southern end of the Sea of Japan. In the GOM, maximum daily cysts fluxes varied from a low of 35 cysts m^{-2} at the SB site to a high of 300,000 cysts m^{-2} at the

WB site, with the maxima at the PB and JB sites being on the order of 100–1000 cysts m^{-2} d^{-1}. The wide spatial variation of toxic *Alexandrium* cyst fluxes observed in the fisheries-rich Gulf of Maine is of significant biological and economic interest when one considers that these data are representative of one dominant species, *A. fundyense*, whereas the Gulf of Naples and Omura Bay studies reported total cyst fluxes for several *Alexandrium* species.

A surprising aspect of the temporal variability in the Gulf of Maine cyst fluxes to the upper traps was that the occurrences of the major cyst export events were rarely if ever coincident with the summer or fall TMF peaks at the sites. This suggests that the delivery of cysts through the water column was decoupled from the predominant, biological particle aggregation mechanisms operating in the upper ocean (e.g., suspension feeding production of detrital and fecal material and aggregation of senescent diatom blooms) which are largely responsible for modulating the total particle mass and POC fluxes (McCave, 1975; Turner and Ferrante, 1979; Honjo et al., 1982; Pilskaln and Honjo, 1987; Alldredge and Silver, 1988; Jackson, 1990; Hill, 1992; MacIntyre et al., 1995; Boyd and Newton, 1999). This was an unexpected finding and implies that the majority of cysts settle individually. Although meso- and micro-zooplankton suspension feeders appear to ingest *Alexandrium* cells in essentially similar proportion to its abundance as an available food item, selective exclusion of the slightly larger 40–50 μm-sized cysts may occur (Bolch et al., 1991; Turriff et al., 1995; Anderson, 1997, 1998; Turner et al., 2000; Doucette et al., 2005; Turner and Borkman, 2005; Turner et al., 2005). Macrobenthic suspension feeders produce fecal pellets containing cysts (Tsujino et al., 2002; Persson et al., 2006) but no quantitative information exists on the occurrence of *Alexandrium* cysts in planktonic zooplankton fecal pellets.

4.2. Bottom resuspension and Alexandrium cyst fluxes

It is clearly evident from the trap data sets that the deep-deployed traps at every GOM site were impacted by prominent particle resuspension. The existence of near-bottom particle resuspension layers, or benthic nepheloid layers, in many locations in the gulf has been noted in several previous studies (Spinrad, 1986; Townsend et al., 1992; Pilskaln et al., 1998; Packard and Christensen, 2004; Kirn et al., 2005; Pilskaln et al., 2014) providing the most spatially extensive data set on GOM BNLs. The persistent, highly elevated deep particle mass fluxes represent a combination of particle delivery from the overlying water column of seasonally variable, biologically produced detrital matter, plus an input of resuspended, fine sedimentary material, resulting in enhanced deep fluxes of all major geochemical component s (e.g., POC, particulate inorganic carbon, biogenic silica and lithogenics; Pilskaln, 2006; Hwang et al., 2009a, 2009b, 2010). Similarly, *Alexandrium* cyst fluxes measured by the BNL-deployed traps were substantially augmented compared to that measured by the upper traps at each site and document the almost year-round presence of cysts in the deeper waters weeks to months after cysts have disappeared from the upper water column. This was particularly apparent at the eastern gulf JB site where the vast majority of the upper water column cyst fluxes were zero but cysts were never absent from the deep trap cups; or at the far western gulf SB site in which the fall-winter, deeper 115 m cyst fluxes were an order of magnitude greater than that at 50 m where minimal to no cysts were collected. Such findings suggest that the BNL is a repository of cysts, delivered from the overlying water column and/or resuspended from bottom sediments. As discussed in

Kirn et al. (2005), cysts suspended in the BNL would be exposed to greater oxygen concentrations and possibly higher temperatures and light levels than cysts buried in the Gulf of Maine sediments and therefore have a higher probability of germination and contribution to the spring bloom planktonic population than sedimentary-bound cysts. Our time-series cyst flux data set documenting the abundance of cysts in near-bottom resuspension layers, even through the winter, lends support to the above hypothesis.

An unresolved issue in the present study, as well as in the Kirn et al. (2005) study in which BNL-suspended cysts were obtained from water samples, is that we do not know exactly what proportion of the cysts suspended in the BNL are resuspended from bottom sediment or are recently formed hypnozygote cysts having settled from overlying waters. Highly elevated deep cyst fluxes at the four sites as compared to that measured in the overlying water column suggests that there must be a subset of the total suspended cyst population in the Gulf of Maine that have a long residence time in the BNL. This deep, suspended cyst population would be enhanced in the summer/early fall months by newly formed cysts sinking out of the upper water column, but not reaching the sediment surface. Additionally, the occurrence of cyst flux peaks in the BNL-deployed traps, which are temporally unrelated to a coincident upper water column cyst flux peak (e.g., JB site in particular), suggests the importance of periodic, near-bottom resuspension events to the overall BNL cyst inventory.

Significant, winter wave energy-driven resuspension of cysts at most of our sites is unlikely as the bottom depths of the sites exceed 100 m. A possible exception may be in the area of northern Stellwagen Bank/at the shallow SB site. Elevated wave and swell energy during fall and winter months might increase bottom shear stress and resuspension of cysts from topographic highs of <100 m located immediately adjacent to the SB mooring. Using the estimates presented in Kirn et al. (2005), it is conceivable that large winter swells of up to 5 m in the gulf could result in sufficient bottom shear stress at depths <100 m to resuspend sediment containing cysts which may in turn be advected into the deeper, SB 115 m trap. Butman et al., (2008) demonstrated that seasonal storm waves of 3–4 m height can result in a bottom stress threshold down to a water depth of 80 m that is adequate to erode and resuspend fine, surficial (0–2 cm) sediments. In particular, the fall 2007 peak in the SB 115 m cyst fluxes with no concurrent cyst flux peak seen in the overlying 50 m trap is indicative of bottom resuspension input.

Based on the time-series flow data presented here, as well as models of bottom shear stress and sediment resuspension produced under varying strengths of tidal, non-tidal, wave and swell-induced currents in coastal systems (Grant and Madsen, 1979; Wright et al., 1986; Glenn and Grant, 1987; Lyne et al., 1990; Souza et al., 2001), we suggest that tidal currents are primarily responsible for the resuspension of sedimentary cysts and likely the maintenance of suspended cysts in the BNL at our sites. Kirn et al. (2005) predicted that bottom tidal currents of approximately 20 cm s^{-1} produce stresses that exceed the critical sediment resuspension threshold for relatively smooth, muddy silt depositional environments which is typical of our study sites (Poppe et al., 2003; Pilskaln, unpublished). Our acoustic flow data from the deep western and eastern Gulf of Maine document the dominance of the near-bottom flow regimes by tidal oscillations between 10–20 cm s^{-1} (mean range). Subtidal flow at 15–25 m above the bottom was substantially less with an

overall mean of 1.5 cm s^{-1}. Cyst fluxes measured by the BNL-deployed traps however displayed only a weak or nonexistent relationship to mean flow speeds per cup sampling interval indicating that the near-bottom, tidally dominated flow regime is not the only factor influencing the deep cyst fluxes. This is not surprising because, as suggested above, factors such as variable BNL residence time of cysts, strong seasonal fluctuations in cyst delivery from the upper water column and incorporation of cysts into sinking biogenic aggregates, plus time-variable excystment rates will all impact the suspended and sinking cyst inventory.

To further examine boundary layer dynamics and the significance of local resuspension to BNL cyst fluxes, we asked the following question: Can we explain the deep, BNL cyst and total particle mass flux using a simple, idealized 1D model? For this exercise, we chose to use Jordan Basin due to the fact that the BNL cyst fluxes were never zero even though upper water column cyst fluxes were frequently zero. Moreover, the TMF in the JB BNL was significantly larger than that measured at the other sites, and the thick JB BNL has been consistently documented as a prominent feature of the basin. Our observations indicate that (1) the mean TMF at 255 m in the JB BNL was 100-fold larger than the mean TMF at 150 m (5 g m^{-2} d^{-1} versus 50 mg m^{-2} d^{-1}), and (2) the mean cyst flux at 255 m was 10-fold greater than that at 150 m (1000 cysts m^{-2} d^{-1} versus 100 cysts m^{-2} d^{-1}). Our hypothesis is that the observed cyst and mass fluxes are consistent with a quasi-steady local one-dimensional balance in which (1) enhanced cyst and mass fluxes within the BNL result from continuous resuspension and deposition that are nearly in balance, and (2) vertical fluxes through the top of the BNL are balanced by net deposition at the bottom. Our boundary layer is the BNL, with the top located at ~155 m as represented in the JB transmissometer profile (Fig. 3), just below the 150 m trap.

Using Rouse (1937), the solution for a steady-state BNL for a single size class of sediment is:

$$\frac{\bar{c}}{c_b}=\left[\frac{(1-\varsigma)/\varsigma}{(1-\varsigma_b)/\varsigma_b}\right]^{v_s/ku_*},\varsigma=\frac{z}{H},\varsigma_b=\frac{b}{H}$$

where c ī̄s the sediment concentration at depth z, c_b ¯is the concentration at a reference depth b, H is the height of the benthic nepheloid boundary layer, V_s is the particle sinking velocity, K is von Karman's constant and u_* is the friction velocity. The friction velocity $u_* \sqrt{\tau/\rho}$ depends on the stress $\tau = C_d \rho u^2$ and can be estimated from the velocity measurements in Jordan Basin which indicate flows of ~15 cm s^{-1} at 255 m, which is 25 m above the bottom (Fig. 4). A typical value of C_d for boundary layer heights on the order of 10 m is 0.001, yielding a friction velocity of 0.005.

With this estimate of the friction velocity, we then ask the question: what particle sinking speed is consistent with the BNL transmissometer profile observed in Jordan Basin (Fig. 3)? The answer is a sinking speed Vs=0.12 cm s^{-1} (Fig. 10a) which corresponds to a particle size of approximately 35 μm (Dietrich, 1982) consistent with that of fine-grained sediments.

The inferred particle sinking speed is a factor of ten higher than laboratory estimates of the sinking speed of *Alexandrium* cysts (10 m d^{-1}, or *Vs*=0.012 cm s^{-1}). As such, we expect the cyst profile to differ dramatically from that of the faster-sinking particles that dominate the TMF and optical properties of the BNL. Indeed, the Rouse model predicts that the concentration of cysts would be much more uniformly distributed in the BNL (Fig. 10b). These differences in the profiles are consistent with the factor of ten difference in the relative increases in total mass and cyst fluxes from just above the boundary layer to within the BNL: there was a 100-fold increase in total mass flux between 150 m and 255 m, whereas the increase in cyst flux was only tenfold.

To summarize, using the measured velocities at 255 m in Jordan Basin and a sinking speed characteristic of the fine-grained sediments present therein, the Rouse model predicts a BNL with an overall shape that resembles transmissometer profiles. Enhancement of total mass and cyst fluxes within the BNL are consistent with continuous resuspension and deposition of material, and the ratio of their relative enhancements is similar to the ratio of particle sinking speeds inferred from the Rouse model. Thus the observed total mass and cyst fluxes observed in Jordan Basin—and by extension, those at our other BNL-dominated sites—can be interpreted in the context of a local one-dimensional balance between modest periodic delivery from the upper water column of newly formed cysts, resuspension, deposition and excystment (germination) (Fig. 11). Indeed, the weak mean subtidal flows at the Jordan Basin site (Fig. 4), together with the tendency of the Jordan Basin Gyre (Brooks and Townsend, 1989; Lynch et al., 1997; Pettigrew et al., 2005) to augment retention of fluid in the basin, favor a local balance.

This does not indicate that lateral fluxes are unimportant—but to a first order, we do not necessarily need to invoke lateral fluxes to explain the observations.

4.3. Variability in eastern versus western Gulf of Maine cyst flux dynamics

The differences between the cyst fluxes at the four sites reflects the major current flow patterns in the gulf, the location of seasonal blooms of *Alexandrium* in the surface waters and the variable impact of cyst resuspension from seedbeds in close proximity to the trap sites. In the far eastern gulf at the JB site, cysts that sink out of the euphotic zone are likely derived from vegetative cells that germinate in the spring from the persistent, high cyst concentration seedbed located at the southeastern edge of the Bay of Fundy (Anderson et al., 2005a; Martin et al., 2005). The cells would be transported out to JB via a segment of the Maine Coastal Current, which flows southwest and forms the northwestern edge of the cyclonic circulation gyre centered over the basin (Brooks and Townsend, 1989; Pettigrew et al., 1998; Townsend et al., 2001; Pettigrew et al., 2005). Although cysts appear to form and settle out periodically in Jordan Basin as documented in the JB 150 m trap, the consistently non-zero, deep cyst fluxes at 255 m point to a much larger source or sources of cysts for the near-bottom water column.

The extreme tidal range of 5 − >16 m in the Bay of Fundy region generates intense tidal mixing and tidal current speeds of 50–150 cm s^{-1} (Bigelow, 1927; Garrett, 1972; Greenberg, 1979; Brooks et al., 1999). Substantial sediment resuspension and lateral transport occurs, driven by the strong tidal flows (Greenberg and Amos, 1983; Wildish and Peer, 1983; Amos

and Mosher, 1985). Several studies have documented high suspended particle transport southward to the mouth of the BOF along the western side, resuspension and lateral advection of tidal mudflat sediments out of the far eastern bays and basins into the open BOF, and the resuspension and tidal movement of organic-rich, fine sediment material from Passamaquoddy Bay into the adjacent BOF (Greenberg and Amos, 1983; Connor et al., 2001; Sutherland et al., 2006). It is probable that such processes lead to the resuspension of cysts which tend to accumulate in silt and clay-rich sediments (Anderson et al., 2005a; Kirn et al., 2005), followed by tidally pulsing of the particle-laden water out of the Bay of Fundy into the MCC and Jordan Basin. This is analogous with the description of the Bay of Fundy as a leaky incubator where *Alexandrium* blooms develop from localized cysts, with vegetative cells from those blooms exiting the bay into the Maine Coastal Current, leading to blooms and toxicity in downstream areas (Anderson et al., 2005a; Martin and White, 1988; McGillicuddy et al., 2005; Townsend et al., 2001). Transects of beam attenuation profiles across the mouth of the Bay of Fundy and offshore into Jordan Basin from the far northeastern Maine coast (Pilskaln et al., 2014), coupled with the JB site tidal current-dominated data, suggest that the BNL cyst population in JB may be fed by flow into the northern edge of the basin of deep, turbid waters from the Bay of Fundy.

The PB site was located within the MCC where a major portion of the current turns offshore, effectively separating the regions of eastern and western Gulf of Maine (Anderson et al., 2005a; Pettigrew et al., 2005). The region is also the site of an extensive sedimentary cyst bed offshore of Penobscot Bay where cyst abundance in the upper 1 cm is consistently high, ranging from 600–2000 cysts cm^{-3} in annual sediment cyst maps produced for 2004–2011 (Anderson et al., 2005a, 2014. The very large deep cyst fluxes at the PB site document the significant tidal resuspension input from the underlying seedbed to the lower water column. This process coupled with the offshore veering or southward directed flow component of the MCC may represent a pathway for cysts to be transported to the Georges Bank region and provide the inoculum for recently documented *Alexandrium* blooms on the bank (Anderson et al., 2005a; McGillicuddy et al., 2014).

The Wilkinson Basin data set, collected on the offshore edge of the MCC and substantially removed from resuspension off western shallow ledges and banks, is most representative of the western gulf particulate and cyst flux dynamics. The tight temporal coupling between large, localized western gulf *Alexandrium* blooms, cyst formation and deep water delivery is significant, contrasting markedly with the lack of temporal coherence between the upper and near-bottom cyst fluxes in the far eastern gulf (e.g., JB).

Throughout the gulf, as represented by our four sites, cysts disappear completely or are present in relatively minimal abundances in the upper water column (e.g., 50–150 m) for periods spanning multiple months. However, there was enormous variability in the cyst flux ranges with median values falling within the lower end of the ranges (Table 2). This suggests that even in regions where extremely high *Alexandrium* surface cell concentrations of 10^4–10^6 cells per liter are observed (Townsend et al. 2001) many cells do not transition into cysts as the massive blooms decline. Regardless, cysts obviously accumulate year to year to produce rich sedimentary seedbeds and provide substantial input to the BNL. Median

BNL cyst fluxes were greatest in the eastern Gulf of Maine and decreased by a factor of seven, east to west (Table 2).

5. Conclusions

Time-series sediment trap data collected at four locations and over several years in the Gulf of Maine document wide spatial and temporal fluctuations in cyst fluxes and highlight the quantitative importance of resuspended cysts to *Alexandrium* population dynamics.

Cyst delivery to sub-euphotic depths was maximal in the summer-early fall and was not temporally coincident with the late summer/fall peaks in total particle mass flux. Our results indicate that the major pulse of cysts through the upper water column is provided by individually sinking cysts with estimated settling at rates of 5–9 m d^{-1}. The western gulf displayed higher magnitude cyst delivery rates from the surface as compared to the eastern gulf, with minimal to no cyst fluxes out of the euphotic zone occurring from late fall through spring in both regions.

Benthic nepheloid layer resuspension was highly prevalent in the Gulf of Maine. It had a significant impact on deep-water *Alexandrium* cyst fluxes which represent a combination of cysts sinking from the surface waters and cysts resuspended from bottom sediments. The latter source appears to be more significant than the former. Cyst fluxes within the BNL were greatest in the eastern gulf and at all sites were substantially elevated compared with the delivery of newly formed cysts out of the upper water column. The cyst flux pattern at the BNL-influenced depths reflected the major summer-early fall cyst export peaks observed in the upper water column and displayed a weak temporal coherence to the total particulate mass flux in the BNL. Tidal current flow was the dominant energy source for benthic cyst resuspension and maintenance of the near-bottom particle resuspension layers at depths of >100 m in the gulf. Ongoing studies are focused on estimating the residence time of cysts in the BNL and bottom sediments in order to determine which cyst repository is the key inoculum source for gulf *Alexandrium* blooms.

Acknowledgments

We are extremely grateful to the captains and crews of the following vessels who made the 5 years of mooring deployments and recoveries in the Gulf of Maine a success: R/V Oceanus, R/V Connecticut, R/V Argo Maine, and F/V Barbara L. Peters. We thank Mooring Systems, Inc., Ocean Data Technologies, Inc., D. Dooner, J. Brown, C. Faulkner, S. Aubrey, J. Wallinga, J. James, D. Percy, B. White, E. Ward and C. White for assistance with mooring design, fabrication and/or at-sea operations. Special thanks to J. Wood for preparation of Aquadopp current meters and data analysis, to D. Handy for providing WHOI dockside operation assistance, to J. Trowbridge and G. Parker for the Rouse model calculations, and to S. Manganini for helping with just about everything. Primary credit for motivating us to examine deep-water cysts fluxes in the Gulf of Maine goes to the late Maureen Keller, a great friend and colleague. We thank two anonymous reviewers for their comments and suggestions which greatly improved the manuscript. This work was supported by NOAA Grant nos. NA04NOS4780274 (ECOHAB-GOM/Cyst) and NA06NOS4780245 (GOMTOX), as well as by research support provided through the Woods Hole Center for Oceans and Human Health, National Science Foundation (NSF) Grant nos. OCE-0430724, and OCE-0911031; and National Institute of Environmental Health Sciences (NIEHS) Grant no. 1-P50-ES012742-01.

References

Alldredge AL, Silver MW. Characteristics, dynamics and significance of marine snow. Prog Oceanogr. 1988; 20:41–81.

Amos CL, Mosher DC. Erosion and deposition of fine-grained sediments from the Bay of Fundy. Sedimentology. 1985; 32:815–832.

Anderson DM. Effects of temperature conditioning on development and germination of *Gonyaulax tamarensis* (Dinophyceae) hynozygote. J Phycol. 1980; 16:166–172.

Anderson DM. Bloom dynamics of toxic *Alexandrium* species in the northeastern US. Limnol Oceanogr. 1997; 42:1009–1022.

Anderson, DM. Physiology and bloom dynamics of toxic Alexandrium species, with emphasis on life cycle transitions. In: Anderson, DM.; Cembella, AD.; Hallegraeff, GM., editors. The Physiological Ecology of Harmful Algal Blooms. Springer-Verlag; Heidelberg: 1998. p. 29-48.

Anderson, DM.; Keafer, BA. Dinoflagellate cyst dynamics in coastal and estuarine waters. In: Anderson, DM.; White, AW.; Baden, DG., editors. Proceedings of the Third International Conference on Toxic Dinoflagellates. Elsevier; New York: 1985. p. 219-224.

Anderson, DM.; Fukuyo, Y.; Matsuoka, K. Cyst methodologies. In: Hallegraeff, GM.; Anderson, DM.; Cembella, AD., editors. Manual on Harmful Marine Microalgae, Monographs on Oceanographic Methodology. Vol. 11. UNESCO; 2003. p. 165-190.

Anderson DM, Kulis DM, Doucette GJ, Gallager JC, Balech E. Biogeography of toxic dinoflagellates in the genus *Alexandrium* from the northeast United States and Canada as determined by morphology, bioluminescence, toxin composition, and mating compatibility. Mar Biol. 1994; 120:467–478.

Anderson DM, Lively JJ, Reardon EM, Price CA. Sinking characteristics of dinoflagellate cysts. Limnol Oceanogr. 1985; 30:1000–1009.

Anderson DM, Stock CA, Keafer BA, Bronzino Nelson A, Thompson B, McGillicuddy DJ, Keller M, Matrai PA, Martin J. *Alexandrium fundyense* cyst dynamics in the Gulf of Maine. Deep-Sea Res II. 2005a; 52 (19–21):2522–2542.

Anderson DM, Townsend DW, McGillicuddy DJ, Turner JT. Deep-Sea Res II. 2005b; 52:2005b, 2365–2368.

Anderson DM, Keafer BA, McGillicuddy DJ, Mickelson MJ, Keay KE, Libby PS, Manning JP, Mayo CA, Whittaker DK, Hickey JM, He R, Lynch DR, Smith KW. Initial observations of the 2005 *Alexandrium fundyense* bloom in southern New England: general patterns and mechanisms. Deep-Sea Res II. 2005c; 52 (19–21):2856–2876.

Anderson DM, Keafer BA, Kleindinst JL, McGillicuddy DJ, Martin JL, Norton K, Pilskaln CH, Smith JL. Alexandrium fundyense cysts in the Gulf of Maine: long-term time series of abundance and distribution, and linkages to past and future blooms. Deep-Sea Res II. 2014; 103:6–26.

Bolch CJ, Blackburn SI, Cannon JA, Hallegraeff GM. The resting cyst of the red-tide dinoflagellate *Alexandrium minutum* (Dinophyceae). Phycologia. 1991; 30 (2):215–219.

Bigelow HB. Plankton of the offshore waters of the Gulf of Maine. Bull US Fish. 1926; 40:1–509.

Bigelow HB. Physical oceanography of the Gulf of Maine. Bulletin US Fish. 1927; 40:511–1027.

Boyd PW, Newton PP. Does planktonic community structure determine downward particle organic carbon flux in different oceanic provinces? Deep-Sea Res I. 1999; 46:63–91.

Brooks DA, Baca MW, Lo YT. Tidal circulation and residence time in a macrotidal estuary: Cobscook Bay, Maine. Estuarine Coastal Shelf Sci. 1999; 49:647–665.

Brooks DA, Townsend DW. Variability of the coastal current and nutrient pathways in the eastern Gulf of Maine. J Mar Res. 1989; 47:303–321.

Butman B, Sherwood CR, Dalyander PS. Northeast storms ranked wind stress and wave-generated bottom stress observed in Massachusetts Bay. Cont Shelf Res. 2008; 28:1231–1245.

Butterworth S. On the theory of filter amplifiers. Wireless Eng. 1930; 7:536–541.

Connor RF, Chmura GL, Beecher B. Carbon accumulation in Bay of Fundy salt marshes: implications for restoration of reclaimed marshes. Global Biogeochem Cycles. 2001; 15:943–954.

Dale, B. Dinoflagellate resting cysts: ‘benthic plankton’. In: Fryxell, GA., editor. Survival Strategies of the Algae. Cambridge University Press; Cambridge: 1983. p. 69-136.

Dietrich EW. Settling velocity of natural particles. Water Resour Res. 1982; 18 (6):1626–1982.

Doucette GJ, Turner JT, Powell CL, Keafer BA, Anderson DM. Trophic accumulation of PSP in zooplankton during *Alexandrium fundyense* blooms in Caaco Bay, Gulf of Maine, April–June

1998. I Toxin levels in *A fundyense* and zooplankton fractions. Deep-Sea Res II. 2005; 52 (19–21): 2764–2783.

Etheridge SM, Roesler CS. Effects of temperature, irradiance and salinity on photosynthesis, growth rates, total toxicity and toxin composition for *Alexandrium fundyense* isolates from the Gulf of Maine and Bay of Fundy. Deep-Sea Res II. 2005; 52 (19–21):2491–2500.

Fugii R, Matsuoka K. Seasonal change of dinoflagellates cyst flux collected in a sediment trap in Omura Bay, West Japan. J Plankton Res. 2006; 28:131–147.

Gardner WD. Sediment trap dynamics and calibration, a laboratory evaluation. J Mar Res. 1980a; 38:17–39.

Gardner WD. Field assessment of sediment traps. J Mar Res. 1980b; 38:41–52.

Garrett C. Tidal resonance in the Bay of Fundy and Gulf of Maine. Nature. 1972; 238:441–443.

Glenn SM, Grant WD. A suspended sediment stratification correction for combined wave and current flows. J Geophys Res. 1987; 92:8244–8264.

Grant WD, Madsen OS. Combined wave and current interaction with a rough bottom. J Geophys Res. 1979; 84:1797–1808.

Greenberg DA. A numerical model investigation of tidal phenomena in the Bay of Fundy and Gulf of Maine. Mar Geodesy. 1979; 2:161–187.

Greenberg DA, Amos CL. Suspended sediment transport and deposition modeling in the Bay of Fundy, Nova Scotia – a region of potential tidal power development. Can J Fish Aquat Sci. 1983; 40 (1):20–34.

He R, McGillicuddy DJ, Keafer BA, Anderson DM. Historic 2005 toxic bloom of *Alexandrium fundyense* in the western Gulf of Maine: 2. coupled biophysical numerical modeling. J Geophys Res. 2008; 113:C07040. http://dx.doi.org/10.1029/2007JC004602.

Hill PS. Reconciling aggregation theory with the observed vertical fluxes following phytoplankton blooms. J Geophys Res. 1992; 97:2295–2308.

Hoagland, P.; Scatasta, S. The economic effects of harmful algal blooms. In: Graneli, E.; Turner, JT., editors. Ecology of Harmful Algae, Ecological Studies. Vol. 189. Springer; New York: 2006. p. 391-402.

Honjo S. Seasonality and interaction of biogenic and lithogenic particulate flux at the Panama Basin. Science. 1982; 218:883–884. [PubMed: 17807141]

Honjo S, Doherty KW. Large aperture time-series sediment traps; design objectives, construction and application. Deep-Sea Res I. 1988; 35:133–149.

Honjo S, Francois R, Manganini S, Dymond J, Collier R. Particle fluxes to the interior of the Southern Ocean in the western Pacific sector along 1708W. Deep-Sea Res II. 2000; 47:3521–3548.

Honjo S, Manganini SJ, Cole JJ. Sedimentation of biogenic matter in the deep ocean. Deep-Sea Res Part I. 1982; 29:608–625.

Hwang J, Montluçon DB, Eglinton TI. Molecular and isotopic constraints on the sources of suspended particulate organic carbon on the northwestern Atlantic margin. Deep-Sea Res. 2009a; 56:1284–1297.

Hwang J, Manganini SJ, Montluçon DB, Eglinton TI. Dynamics of particle export on the Northwest Atlantic margin. Deep-Sea Res. 2009b; 56:1792–1803.

Hwang J, Druffel ERM, Eglinton TI. Widespread influence of resuspended sediments on oceanic particulate organic carbon: Insights from radiocarbon and aluminum contents in sinking particles. Global Biogeochem Cycles. 2010; 24:GB4016. <http://dx.doi.org/10.1029/2010GB003802>.

Jackson GA. A model of the formation of marine algal flocs by physical coagulation processes. Deep-Sea Res Part I. 1990; 37:1197–1211.

Keafer BA, Churchill J, Anderson DM. Blooms of the toxic dinoflagellate, *Alexandrium fundyense*, in the Casco Bay region of the western Gulf of Maine: advection from offshore source populations and interactions with the Kennebec River plume. Deep-Sea Res II. 2005a; 52 (19–20):2631–2655.

Keafer BA, Churchill JH, McGillicuddy DJ, Anderson DM. Bloom development and transport of toxic *Alexandrium fundyense* populations within a coastal plume in the Gulf of Maine. Deep-Sea Res II. 2005b; 52 (19–21):2674–2697.

Kirn SL, Townsend DW, Pettigrew NR. Suspended *Alexandrium* spp. hypnozygote cysts in the Gulf of Maine. Deep-Sea Res II. 2005; 52 (19–21):2543–2559.

Lewis, CM.; Yentsch, CM.; Dale, B. Distribution of *Gonyaulax excavata* resting cysts in the sediments of Gulf of Maine. In: Taylor, BL.; Seliger, HH., editors. Dev Marine Biol; Toxic dinoflagellate blooms. Proceedings of the Second International Conference on Toxic Dinoflagellate Blooms; Elsevier; 1979. p. 235-238.

Li Y, He R, McGillicuddy DJ, Anderson DM, Keafer BA. Investigation of the 2006 *Alexandrium fundyense* bloom in the Gulf of Maine: In-situ observations and numerical modeling. Cont Shelf Res. 2009; 29:2069–2082.

Love RC, Loder TC, Keafer BA. Nutrient conditions during *Alexandrium fundyense* blooms in the western Gulf of Maine. Deep-Sea Res II. 2005; 52 (19–21):2450–2466.

Lynch DR, Holbrook MJ, Naimie CE. The Maine coastal current: spring climatological circulation. Cont Shelf Res. 1997; 17:605–634.

Lyne VD, Butman B, Grant WD. Sediment movement along the US east coast continental shelf: I. Estimates of bottom stress using the Grant-Madsen model and near-bottom wave and current measurements. Cont Shelf Res. 1990; 13:397–428.

MacIntyre S, Alldredge AL, Gotschalk CC. Accumulation of marine snow at density discontinuities in the water column. Limnol Oceanogr. 1995; 40:449–468.

Martin JL, White AW. Distribution and the abundance of the toxic dinoflagellate *Gonyaulax excavata* in the Bay of Fundy. Can J Fish Aquat Sci. 1988; 45:1968–1975.

Martin JL, Page FH, Hanke A, Strain PM, LeGresley MM. *Alexandrium fundyense* vertical distribution patterns during 1982, 2001 and 2002 in the offshore Bay of Fundy, eastern Canada. Deep-Sea Res II. 2005; 52 (19–21):2569–2592.

Matrai P, Thompson B, Keller M. *Alexandrium* spp. from eastern Gulf of Maine populations: Circannual excystment. Deep-Sea Res II. 2005; 52 (19–21):25602568.

McCave IN. Vertical flux of particles in the ocean. Deep-Sea Res I. 1975; 22:491–502.

McGillicuddy DJ, Signell RP, Stock CA, Keafrer BA, Keller MD, Hetland RD, Anderson DM. A mechanism for offshore initiation of harmful algal blooms in the coastal Gulf of Maine. J Plankton Res. 2003; 25:1131–1138.

McGillicuddy DJ, Anderson DM, Lynch DR, Townsend DW. Mechanisms regulating large-scale seasonal fluctuations in *Alexandrium fundyense* populations in the Gulf of Maine: results from a physical–biological model. Deep-Sea Res II. 2005; 52 (19–21):2698–2714.

McGillicuddy DJ, Townsend DW, Keafer BA, Thomas MA, Anderson DM. Georges Bank: a leaky incubator of *Alexandrium fundyense* blooms. Deep-Sea Res II. 2014; 103:163–173.

Montresor M, Zingone A, Sarno D. Dinoflagellate cyst production at a coastal Mediterranean site. J Plankton Res. 1998; 20:2291–2312.

Packard TT, Christensen JP. Respiration and vertical carbon flux in the Gulf of Maine water column. J Mar Res. 2004; 62:93–115.

Passow U, De La Rocha CL. Accumulation of mineral ballast on organic aggregates. Global Biogeochem Cycles. 2006; 20 210.1029/2005GB002579.

Pershing AJ, Greene CH, Jossi JW, O'Brien L, Brodziak J, Bailey BA. Interdecadal variability in the Gulf of Maine zooplankton community with potential impacts on fish recruitment. ICES J Mar Sci. 2005; 62:1511–1523.

Persson A, Smith BC, Wikfors GH, Quilliam M. Grazing on toxic *Alexandrium fundyense* resting cysts and vegetative cells by the eastern oyster (*Crassostrea virginica*). Harmful Algae. 2006; 5:678–684.

Pettigrew NR, Townsend DW, Xue H, Wallinga JP, Brickley PJ, Hetland RD. Observations of the eastern Maine coastal current and its offshore extensions in 1994. J Geophys Res. 1998; 103 (623–30):639.

Pettigrew NR, Churchill JH, Janzen CD, Mangum LJ, Signell RP, Thomas AC, Townsend DW, Wallinga JP, Xue X. The kinematic and hydrographic structure of the Gulf of Maine coastal current. Deep-Sea Res II. 2005; 52 (19–21):2369–2391.

Pilskaln, CH. Seasonal and interannual biogeochemical particle flux dynamics in the Gulf of Maine. Proceedings of the Gulf of Maine Symposium on Advancing Ecosystem Research for the Future of the Gulf; New Brunswick, Canada. 2009. p. 84Program of Abstracts

Pilskaln CH, Honjo S. The fecal pellet fraction of biogeochemical particle fluxes to the deep sea. Global Biogeochem Cycles. 1987; 1:31–48.

Pilskaln, CH.; Paduan, JB. Monterey Bay Aquarium Research Institute (MBARI) Technical Report 92-9. 1992. Laboratory techniques for the handling and geochemical analysis of water column particulate and surface sediment samples; p. 22

Pilskaln CH, Churchill JH, Mayer LM. Resuspension of sediment by bottom trawling in the Gulf of Maine and potential geochemical consequences. J Conserv Biol. 1998; 12:1223–1230.

Pilskaln, CH.; Anderson, D.; Keafer, B.; Townsend, D. The Gulf of Maine benthic nepheloid layer: particle characterization, dynamics, and transformations. AGU/ASLO Ocean Sciences Meeting, EOS Transactions 87; 2006. p. 120p

Pilskaln CH, Lehmann C, Paduan JB, Silver MW. Spatial and temporal dynamics in marine aggregate abundance, sinking rate and flux: Monterey Bay, central California. Deep-Sea Res II. 1998; 45:1803–1837.

Pilskaln CH, Hayashi K, Keafer BA, Anderson DM. Benthic nepheloid layers in the Gulf of Maine and *Alexandrium fundyense* cyst inventories. Deep-Sea Res II. 2014; 103:55–65.

Pilskaln CH, Paduan JB, Chavez FP, Anderson RY, Berelson WM. Carbon export and regeneration in the coastal upwelling system of Monterey Bay, central California. J Mar Res. 1996; 54:1149–1178.

Pilskaln CH, Manganini SJ, Asper VL, Trull TW, Howard W, Armand L, Massom R. Biogeochemical particle fluxes in the Indian Sector of the Southern Ocean: 1998–2001. Deep-Sea Res I. 2004; 51:307–322.

Poppe, LJ.; Paskevich, VF.; Williams, SJ.; Hastings, ME.; Kelley, JT.; Belknap, DF.; Ward, LG.; FitzGerald, DM.; Larsen, PF. US Geological Survey Open-File Report 03-001. 2003. Surficial sediment data from the Gulf of Maine, Georges Bank, and Vicinity: A GIS compilation.

Rouse H. Modern concepts of the mechanics of turbulence. Trans Am Soc Civil Eng. 1937; 102:463–543.

Shumway SE, Sherman-Caswell S, Hurst JW. Paralytic shellfish poisoning in Maine: monitoring a monster. J Shellfish Res. 1988; 7 (4):643–652.

Siegel DA, Deuser WG. Trajectories of sinking particles in the Sargasso Sea: modeling of statistical funnels above deep-ocean sediment traps. Deep-Sea Res. 1997; 9:1519–1541.

Souza AJ, Dickey TD, Chang GC. Modeling water column structure and suspended particulate matter on the Middle Atlantic continental shelf during the passages of Hurricanes Edouard and Hortense. J Mar Res. 2001; 59:1021–1045.

Spinrad RJ. An optical study of the water masses of the Gulf of Maine. J Geophys Res. 1986; 91:1007–1018.

Sutherland EM, Gobas FAPC, Branfireun BA, Heyes A. Environmental controls on the speciation and distribution of mercury in coastal sediments. Mar Chem. 2006; 102:111–123.

Thomas AC, Townsend DW, Weatherbee R. Satellite-measured phytoplankton variability in the Gulf of Maine. Cont Shelf Res. 2003; 23:971–989.

Townsend DW. Influences of oceanographic processes on the biological productivity of the Gulf of Maine. Rev Aquat Sci. 1991; 5 (3–4):211–230.

Townsend, DW.; Ellis, WG. Primary production and nutrient cycling on the Northwest Atlantic continental shelf. In: Liu, KK.; Atkinson, L.; Quinones, R.; Talaue-McManus, L., editors. Carbon and Nutrient Fluxes in Continental Margins: A Global Synthesis. Springer-Verlag; New York: 2009. p. 234-248.

Townsend DW, Mayer LM, Dortch LM, Spinrad RWQ. Vertical structure and biological activity in the bottom nepheloid layer of the Gulf of Maine. Cont Shelf Res. 1992; 12:367–387.

Townsend DW, Pettigrew NR, Thomas AC. Offshore blooms of the red tide dinoflagellate, *Alexandrium* sp., in the Gulf of Maine. Cont Shelf Res. 2001; 21:347–369.

Townsend DW, Pettigrew NR, Thomas AC. On the nature of *Alexandrium fundyense* blooms in the Gulf of Maine. Deep-Sea Res II. 2005; 52 (19–21):2603–2630.

Townsend DW, Rebuck ND, Thomas MA, Karp-Boss L, Gettings RM. A changing nutrient regime in the Gulf of Maine. Cont Shelf Res. 2010; 30:820–832.

Tsujino M, Kamiyama T, Uchida T, Yamaguchi M, Itakura S. Abundance and germination capability of resting cysts of *Alexandrium* spp. (Dinophyceae) from faecal pellets of macrobenthic organisms. J Exp Mar Bio Ecol. 2002; 271:1–7.

Turner JT, Ferrante JA. Zooplankton fecal pellets in aquatic ecosystems. Bioscience. 1979; 29:670–677.

Turner JT, Doucette GJ, Powell CL, Kulis DM, Keafer BA, Anderson DM. Accumulation of red tide toxins in larger size fractions of zooplankton assemblages from Massachusetts Bay, USA. Mar Ecol Prog Ser. 2000; 203:95–107.

Turner JT, Borkman DG. Impact of zooplankton grazing on *Alexandrium* spp. in the offshore Gulf of Maine. Deep-Sea Res II. 2005; 52 (19–21):2801–2816.

Turner JT, Doucette GJ, Keafer BA, Anderson DM. Trophic accumulation of PSP in zooplankton during *Alexandrium fundyense* blooms in Caaco Bay, Gulf of Maine, April–June 1998. II Zooplankton abundance and size-fractionated community composition. Deep-Sea Res II. 2005; 52 (19–21):2784–2800.

Turriff N, Runge JA, Cembella AD. Toxin accumulation and feeding behaviour of the planktonic copepod *Calanus finmarchicus* exposed to the red-tide dinoflagellate *Alexandrium excavatum*. Mar Biol. 1995; 123:55–64.

White AW, Lewis CM. Resting cysts of the toxic, red tide dinoflagellate Gonyaulax excavata in Bay of Fundy sediments. Can J Fish Aquat Sci. 1982; 39:1185–1194.

Wildish DJ, Peer D. Tidal current speed and production of benthic macrofauna in the lower Bay of Fundy. Can J Fish Aquat Sci. 1983; 40 (1):309–321.

Wright LD, Boon JD III, Green MO, List JH. Response of the mid shoreface of the southern Mid-Atlantic Bight to a “Northeaster. Geo-Mar Lett. 1986; 6:153–160.

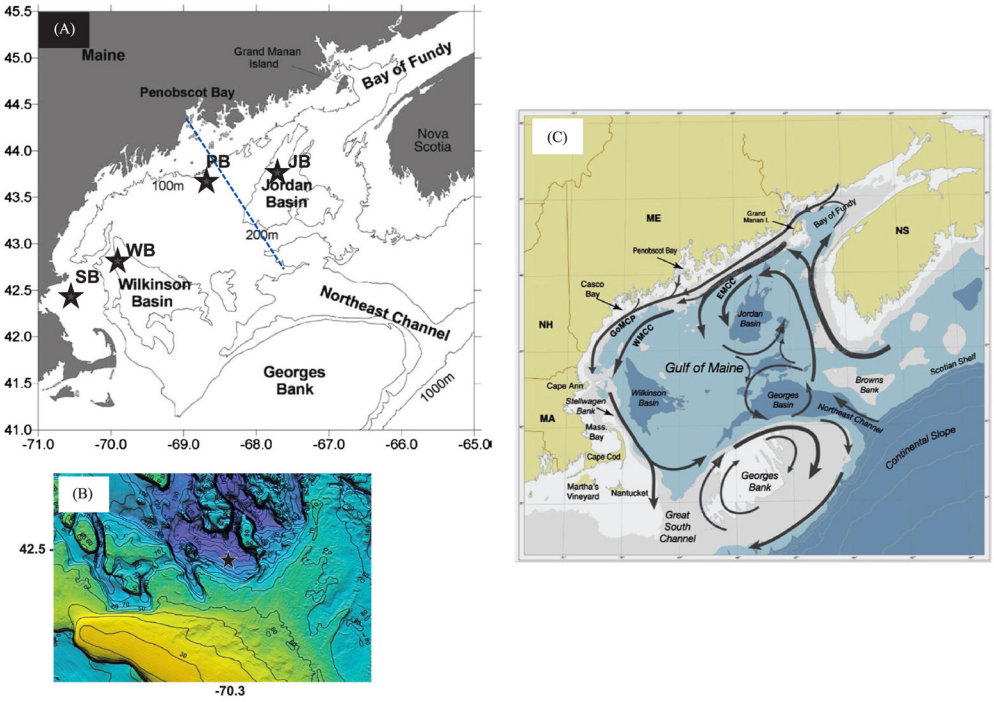

Fig. 1.

(A) Gulf of Maine study region with major bathymetric features and subsurface sediment trap mooring locations (black stars): SB-northern Stellwagen Bank (2007–2008), WB-Wilkinson Basin (2008–2010), PB-offshore Penobscot Bay (2005–2006) and JB-Jordan Basin (2005–2006). Blue dashed cross-shelf line indicates boundary between western and eastern gulf regions. Trap depths and exact deployment periods given in Table 1. (B) Detailed bathymetry of SB site within small basin on northern edge of Stellwagen Bank (courtesy USGS, Woods wHole, MA); black star indicates mooring site. (C) Schematic circulation diagram for major currents in the Gulf of Maine (from Anderson et al. (2005b); EMCC=Eastern Maine Coastal Current; WMCC=Western Maine Coastal Current; GoMCP=Gulf of Maine Coastal Plume).

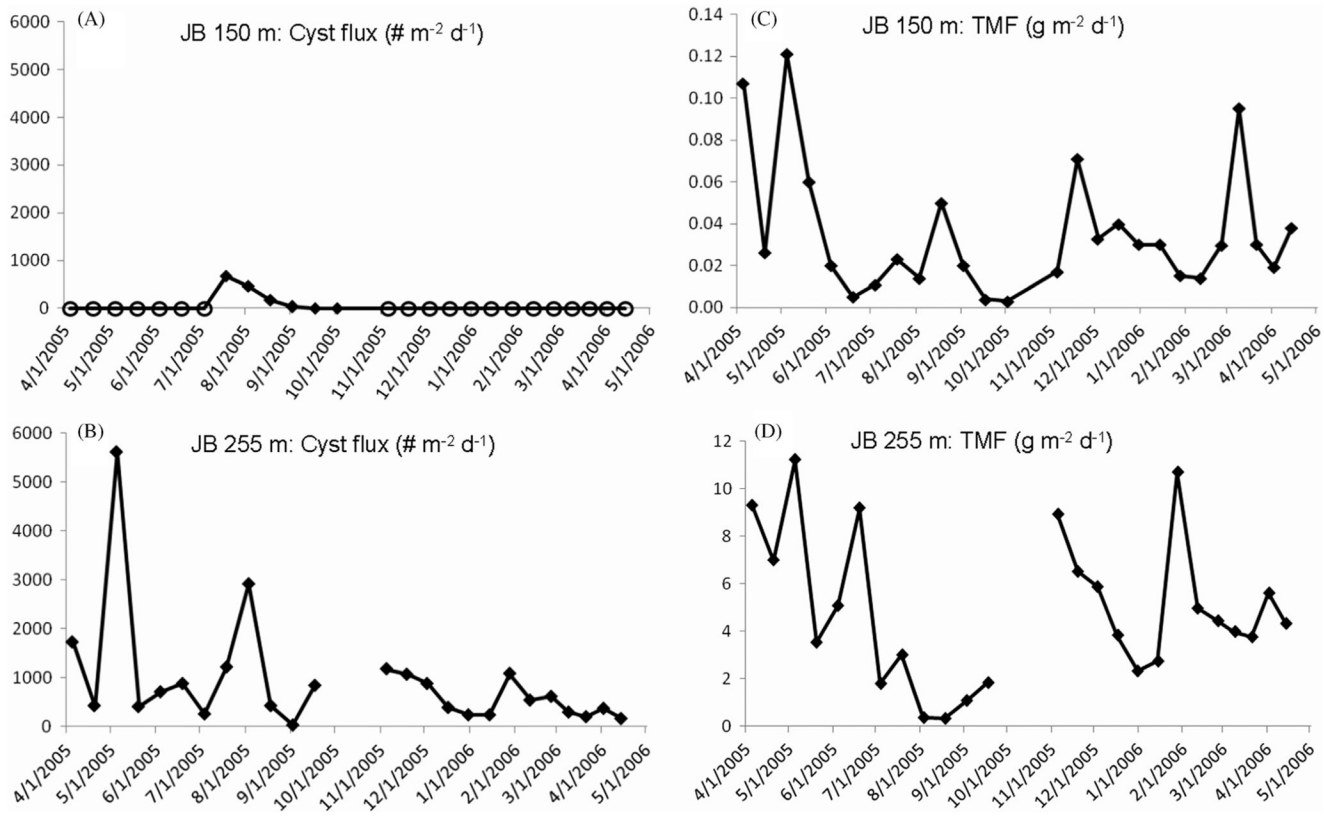

Fig. 2.

Jordan Basin site, April 2005–May 2006 cyst and total mass fluxes of particulates (TMF). (A) Cyst fluxes (# m^{-2} d^{-1}) measured at 150 m and (B) at 255 m. Open circle marker symbols indicate zero cyst flux/no cysts collected in the trap cup during the particular collection period. (C) TMF measured at JB 150 m and (D) at JB 255 m, both in g m^{-2} d^{-1}. Breaks in 255 m cyst and TMF plot lines indicates lost trap sample due to trap malfunction.

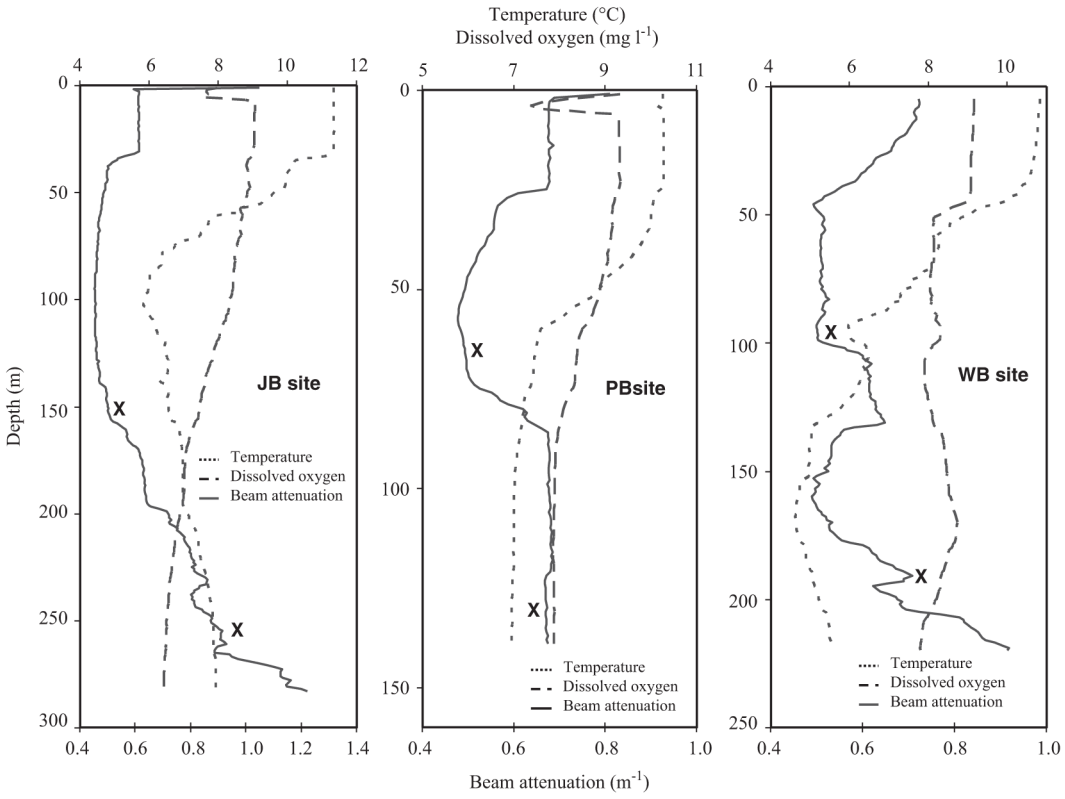

Fig. 3.

Representative depth profiles obtained during the month of October (2005, 2006, 2008) of temperature (0 °C), dissolved oxygen (mg l^{-1}) and beam attenuation (m^{-1}) at the JB, PB and WB mooring sites.

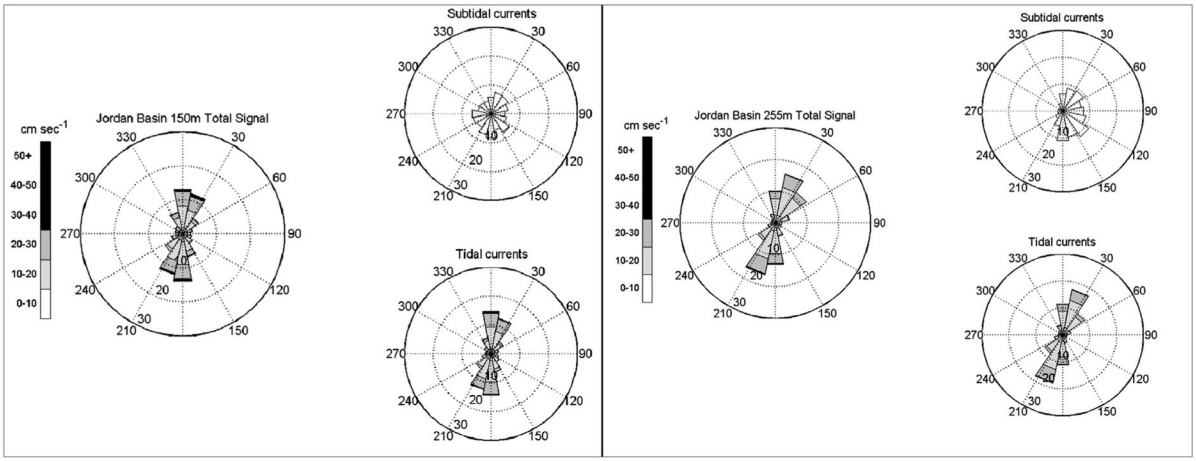

Fig. 4.

Jordan Basin mooring site current speeds and direction at 150 m and 255 m for deployment period August–May 2005. Rose diagrams present flow speeds and direction for the total flow signal, subtidal and tidal signals at each depth. Flow direction is indicated by the shaded, 22.5° slices or petals; cm s^{-1} flow speeds are indicated by scale bar to the left of each set of diagrams. The percentage of time measured flows fell within a specific direction and velocity bin is indicated by the annular circles of the rose diagrams.

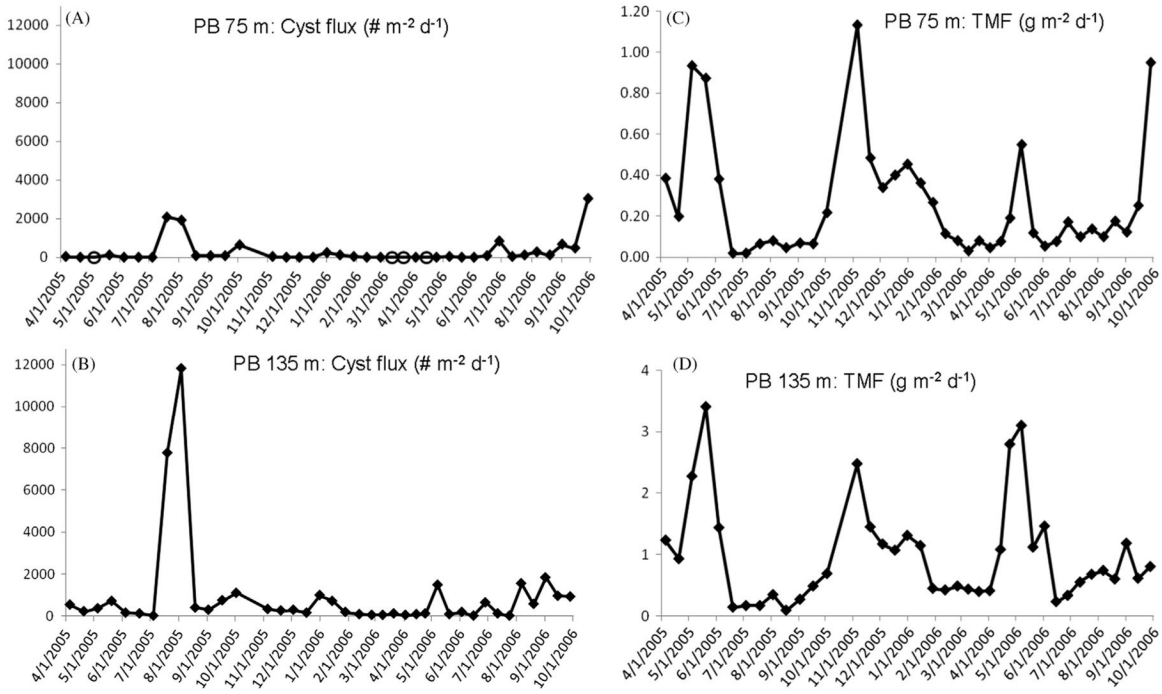

Fig. 5.

Offshore Penobscot Bay (PB) site, April 2005–October 2006 cyst and total mass fluxes of particulates (TMF). (A) Cysts fluxes (# m^{-2} d^{-1}) measured at 75 m and (B) at 135 m. Open circle marker symbols in (A) indicate zero cyst flux/no cysts collected in the trap cup during the particular collection period. Note that range scale of cyst fluxes was 0–10^3 cysts m^{-2} d^{-1} at 75 m and 10^2–10^4 m^{-2} d^{-1}. (C) TMF measured at PB 75 m and (D) at PB 135 m, both in g m^{-2} d^{-1}.

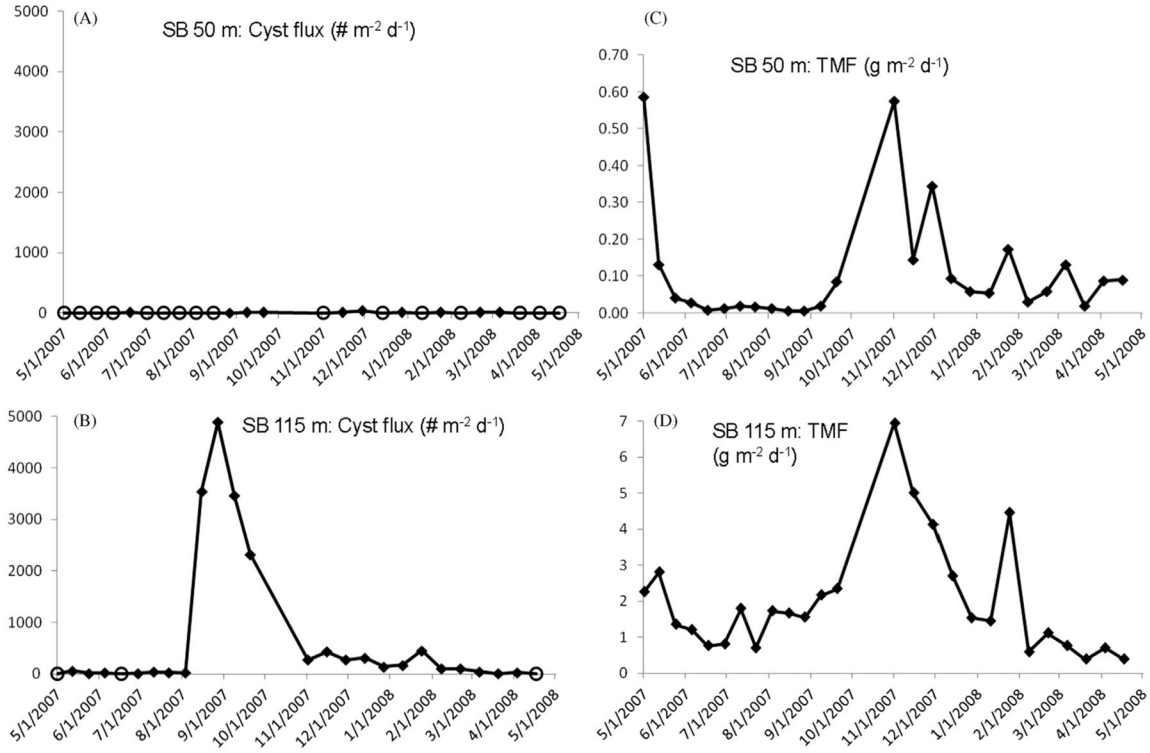

Fig. 6.

Northern Stellwagen Bank (SB) site, May 2007–May 2008 cyst and total mass fluxes of particulates (TMF). (A) Cysts fluxes (# m^{-2} d^{-1}) measured at the, 50 m and (B) 115 m. Open circle marker symbols in (A) and (B) indicate zero cyst flux/no cysts collected in the trap cup during the particular collection period. Note that the range scale of cyst fluxes was 0–10^1 cysts m^{-2} d^{-1} at 50 m and 0–10^3 cysts m^{-2} d^{-1} at 115 m. (C) TMF measured at SB 50 m and (D) at SB 115 m, both in g m^{-2} d^{-1}.

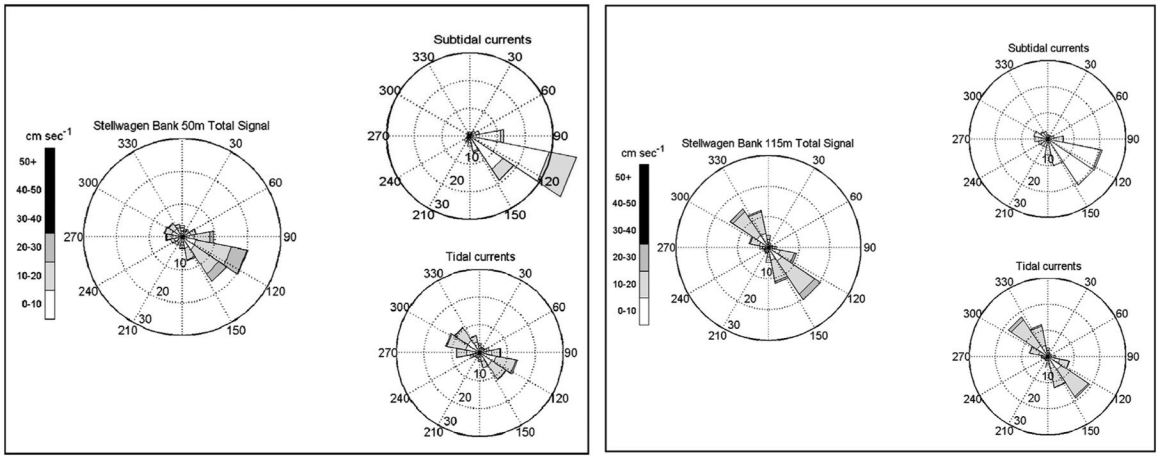

Fig. 7.

Northern Stellwagen Bank mooring site current speeds and direction at 50 m and 115 m for deployment period May 2007–April 2008. Refer to Fig. 4 for detailed diagram explanation.

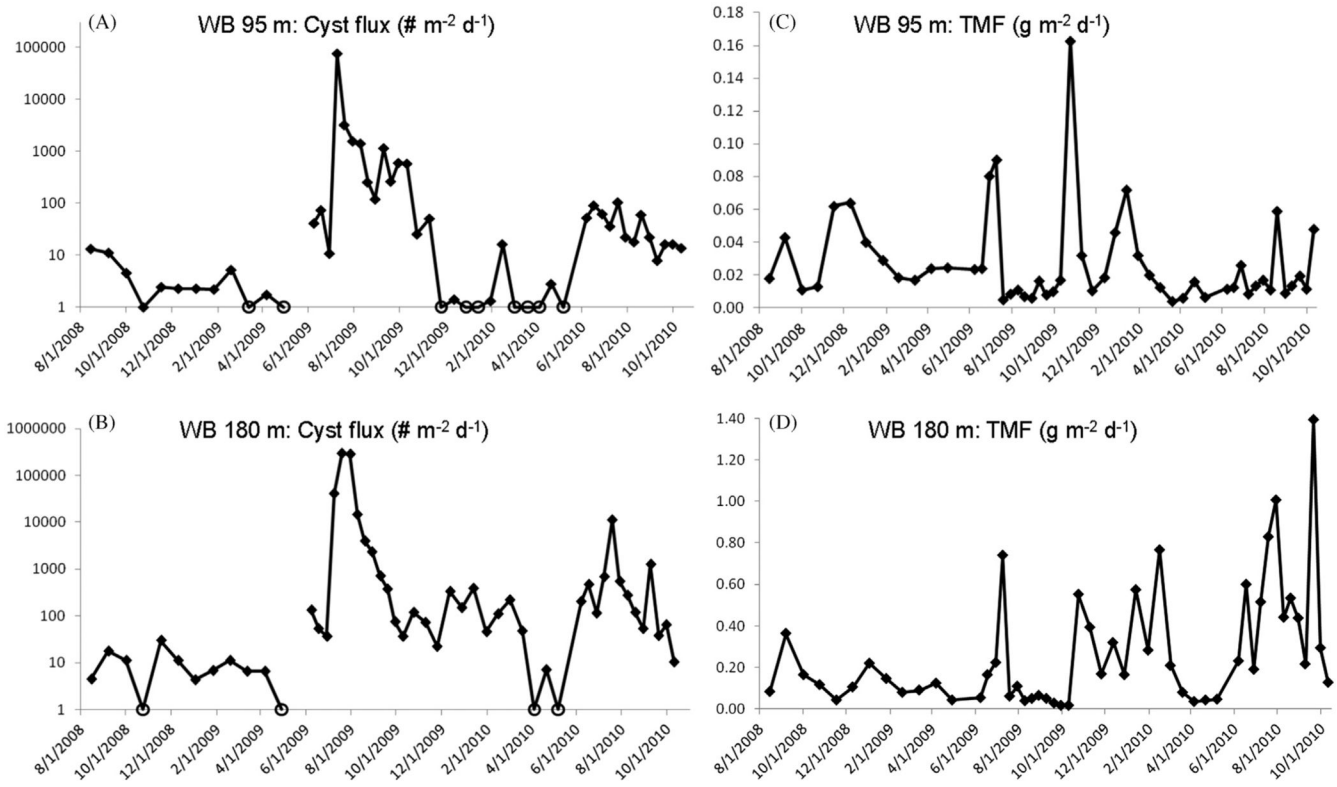

Fig. 8.

Northern Wilkinson Basin (WB) site, August 2008–October 2010 cyst and total mass fluxes of particulate material (TMF). (A) Cysts fluxes (# m^{-2} d^{-1}) measured at the, 95 m and (B) at 180 m. Open circle marker symbols in (A) and (B) indicate zero cyst flux/no cysts collected in the trap cup during the particular collection period. (C) TMF measured at WB 95 m and (D) WB 180 m, both in g m^{-2} d^{-1}.

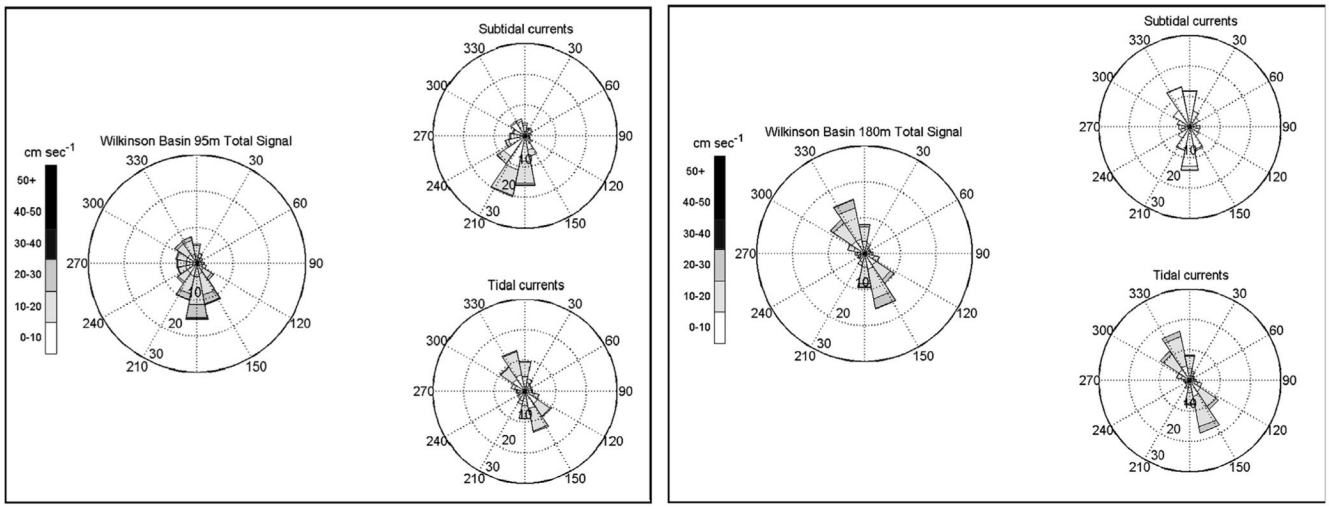

Fig. 9.

Wilkinson Basin mooring site current speed and direction at 95 m and 180 m for deployment period August 2008–June 2010. Refer to Fig. 4 for detailed diagram explanation.

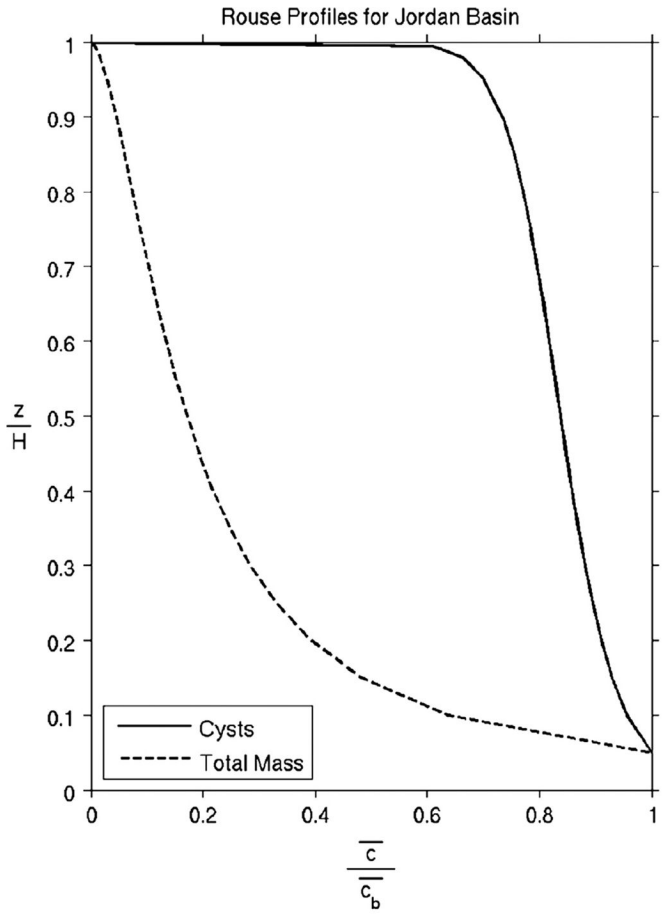

Fig. 10.

Rouse (1937) model profiles for Jordan Basin BNL (see text for factor definitions). Solid line: particle sinking speed of 0.12 cm s^{-1} for total mass fluxes, JB 255 m; dashed line: laboratory-measured cyst sinking speed of 0.012 cm s⁻1 (Anderson et al., 1985). Both profiles reach their reference concentrations at 0.05 of the boundary layer height. Rouse profile calculations made with the algorithm available at <http://vtchl.uiuc.edu/people/parkerg/excel_files.htm>.

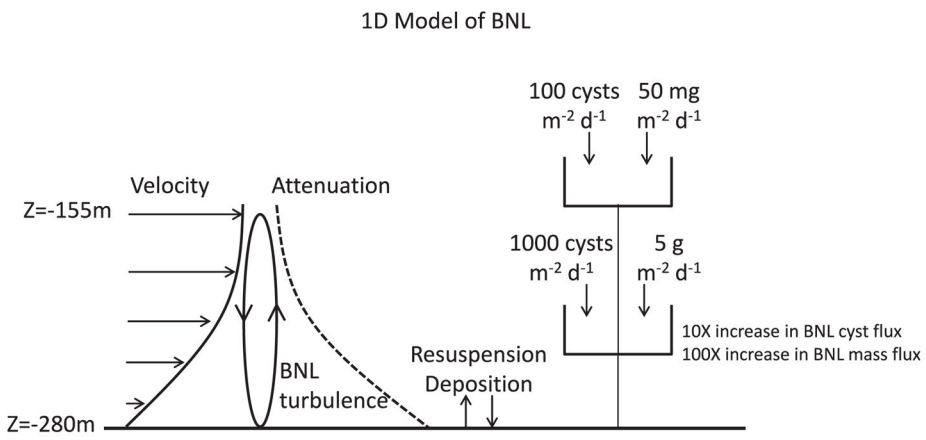

Fig. 11.

Cyst and total mass fluxes in Jordan Basin: Idealized 1D model based on Rouse (1937). Top of boundary layer (BNL) is 155 m based on JB transmissometer profiles.

Table 1

Gulf of Maine subsurface sediment trap moorings, 2005–2010.

Mooring site	Location	Deployment period	Trap depths (m)	Bottom depth (m)
JB (Jordan Basin)	43 29.9N; 67 50.3W	April 2005–April 2006	150, 255	280
PB (offshore Penobscot Bay)	43 36.2N; 68 43.6W	April 2005–October 2006	75, 135	150
SB (northern Stellwagen Bank)	42 28.2N; 70 18.4W	May 2007–April 2008	50, 115	130
WB (Wilkinson Basin)	42.71N; 69.96W	August 2008–November 2010	95, 180	200

Table 2

Summary of minimum, maximum and median *Alexandrium fundyense* cyst fluxes (# m^{-2} d^{-1}) at four Gulf of Maine sediment trap sites.

Mooring site/trap depth	Minimum	Maximum	Median
JB/150 m	0	676	0
JB/255 m	35	5616	496
PB/75 m	0	3037	58
PB/135 m	18	11,806	287
SB/50 m	0	34	0
SB/115 m	0	4887	79
WB/95 m	0	78,236	16
WB/180 m	0	292,894	72